

Influence of isothermal annealing on the critical behaviour of amorphous $\text{Fe}_{90+x}\text{Zr}_{10-x}$ alloys

This article has been downloaded from IOPscience. Please scroll down to see the full text article.

1991 J. Phys.: Condens. Matter 3 2703

(<http://iopscience.iop.org/0953-8984/3/16/009>)

View [the table of contents for this issue](#), or go to the [journal homepage](#) for more

Download details:

IP Address: 171.66.16.151

The article was downloaded on 11/05/2010 at 07:12

Please note that [terms and conditions apply](#).

Influence of isothermal annealing on the critical behaviour of amorphous $\text{Fe}_{90+x}\text{Zr}_{10-x}$ alloys

S N Kaul and Ch V Mohan

School of Physics, University of Hyderabad, Central University PO, Hyderabad-500 134, India

Received 8 October 1990

Abstract. Extensive ferromagnetic resonance (FMR) measurements have been performed in the critical region on amorphous $\text{Fe}_{90}\text{Zr}_{10}$ and $\text{Fe}_{91}\text{Zr}_9$ alloys before and after they have undergone isothermal annealing at 400 K for durations of time ranging from 10 to 240 min. Saturation magnetization M_s and resonance field H_{res} as functions of temperature in the critical region are accurately determined by a detailed lineshape analysis of the observed FMR spectra. The ‘range-of-fit’ scaling-equation-of-state analysis is then employed to arrive at the asymptotic values of the spontaneous magnetization and initial susceptibility critical exponents β and γ from the $M_s(H_{\text{res}}, T)$ data so obtained. Isothermal annealing causes a significant enhancement in the Curie temperature T_C , but leaves the values of the exponents β and γ , which are fairly close to those predicted by the three-dimensional Heisenberg model, unaltered. The FMR linewidth versus temperature curves exhibit an abrupt slope change at T_C , indicating a well-defined phase transition from the ferromagnetic to the paramagnetic state.

1. Introduction

Amorphous $\text{Fe}_{100-x}\text{Zr}_x$ (a- $\text{Fe}_{100-x}\text{Zr}_x$) alloys exhibit a complex magnetic behaviour in the Zr concentration range $7 \leq x \leq 12$. While the observations (Ryan *et al* 1987) such as firstly a *decrease* in the Curie temperature T_C (from 265.5 K for $x = 12$ to 163 K for $x = 7$) and magnetic moment, μ_{Fe} per Fe atom (from $1.6 \mu_B$ for $x = 12$ to $0.58 \mu_B$ for $x = 7$) with x , secondly failure of magnetization to saturate in fields up to 190 kOe and a large high-field susceptibility at 4.2 K which *increases* with *decreasing* x , and thirdly a finite (about 100 Å) spin–spin correlation length ξ (Rhyne *et al* 1988) at $T < T_C$ have been taken to suggest that a long-range ferromagnetic (FM) ordering does not develop at any temperature and T_C marks a transition to an unconventional FM state (described as a ‘wandering-axis’ ferromagnet (Ryan *et al* 1987) or equivalently as a strongly exchange-frustrated spin system in which the FM correlations are short ranged (Rhyne *et al* 1988), $\xi \approx 100$ Å), a sharp singularity at T_C in ‘zero-field’ susceptibility (Kaul *et al* 1986, Saito *et al* 1986, Kaul 1987) and temperature derivative of electrical resistivity (Kaul *et al* 1990) characterized by three-dimensional (3D) Heisenberg-like critical exponents (Kaul *et al* 1986, 1990, Kaul 1987, 1988) and a host of other properties (Kaul *et al* 1988, Kaul and Siruguri 1991) find an adequate description (Kaul 1988, Kaul *et al* 1988, Kaul and Siruguri 1991) in terms of the *infinite*-3D-FM-matrix plus *finite*-spin-clusters picture (Kaul 1984, 1985). Now that the alloys in question are known (Shirakawa *et al* 1980, Ryan *et al* 1987)

to behave as good soft ferromagnets (i.e. they readily saturate in fields of 1 kOe or higher with no measurable high-field slope) with T_C in excess of 400 K and $\mu_{Fc} \approx 2\mu_B$ upon hydrogenation (Ryan *et al* 1987) or replacement (Shirakawa *et al* 1980) of even a small amount of Fe by Co or Ni, either of these treatments should *drastically* affect the critical behaviour of a 'wandering-axis ferromagnet' whereas they should leave the critical behaviour *unaltered* if the spin structure of the parent alloys corresponds to the infinite-3D-FM-matrix plus finite-spin-clusters description. Thus, a detailed study of the critical behaviour of a-Fe_{90-x}(Co, Ni)_xZr₁₀ and a-Fe_{100-x}Zr_xH_y alloys provides a decisive means of ascertaining which of the above-mentioned descriptions is correct. We have recently carried out such a study on a-Fe_{90-x}Co_xZr₁₀ ($x = 0, 1, 2$ and 4) alloys with the result that substitution of Fe by Co has *no effect* (Kaul and Babu 1991) on the 3D Heisenberg-like critical behaviour of the parent alloy (i.e. the alloy with $x = 0$). A similar investigation on a-Fe_{100-x}Zr_xH_y alloys is, however, made impossible by the desorption of hydrogen for temperatures in the vicinity of T_C . Realizing that the effects similar to those caused by hydrogenation can also be induced by structural relaxation consequent upon annealing treatment and that the ferromagnetic resonance (FMR) technique offers a new but powerful tool (Kaul and Babu 1991) for investigating the critical behaviour of ferromagnets, detailed FMR measurements have been performed in the critical region on a-Fe_{90+x}Zr_{10-x} ($x = 0$ and 1) alloys before and after subjecting them to isothermal annealing at $T_A = 400$ K for different time durations, t_A ranging from 10 to 240 min in a high-purity nitrogen gas atmosphere.

2. Experimental results and data analysis

The microwave power P absorption derivative, dP/dH was measured as a function of the external static magnetic field H on strips 4 mm long (cross section, about 2 mm \times 0.03 mm) cut from the alloy ribbons coming from the same batch as that used in our earlier investigations (Kaul *et al* 1986, 1990, Kaul 1987), using horizontal-parallel \parallel^h and vertical-parallel \parallel^v sample configurations (in which H is directed either along the length or along the breadth in the ribbon plane) at a fixed microwave field frequency $\nu = \omega/2\pi \approx 9.228$ GHz, in the temperature range $-0.1 \leq \varepsilon = (T - T_C)/T_C \leq 0.1$ at 0.5 K intervals. The sample temperature was monitored with a pre-calibrated copper-constantan thermocouple and held constant to within ± 50 mK at every temperature setting. The details concerning the temperature measurement and control have been given in our previous reports (Kaul and Babu 1991, Kaul and Siruguri 1991). The FMR data taken on strips cut from different parts of the alloy ribbon and on the same alloy strip during different experimental runs establish that the resonance field H_{res} (defined as the field where the $dP/dH = 0$ line cuts the dP/dH versus H curve) and the 'peak-to-peak' linewidth ΔH_{pp} are reproduced to within $\pm 1\%$ and $\pm 10\%$, respectively.

In order to put the present findings in a proper context, a brief mention needs to be made of our previous observations (Kaul and Siruguri 1991) as follows.

(i) The FMR spectra taken at $T \approx T_C$ for a-Fe₉₀Zr₁₀ and a-Fe₉₁Zr₉ alloys consist of a single resonance (primary resonance) but, as the temperature is raised through T_C , the signature of another resonance (secondary resonance), first noticed at a lower field value of about 800 Oe for $T = T_C$ in the most sensitive setting of the spectrometer, gives way to a full-fledged resonance for $T \geq T_C + 10$ K whereas the primary resonance shifts to higher fields and broadens out so much that it is hardly discernible for $T \geq 350$ K and leaves behind a well resolved secondary resonance.

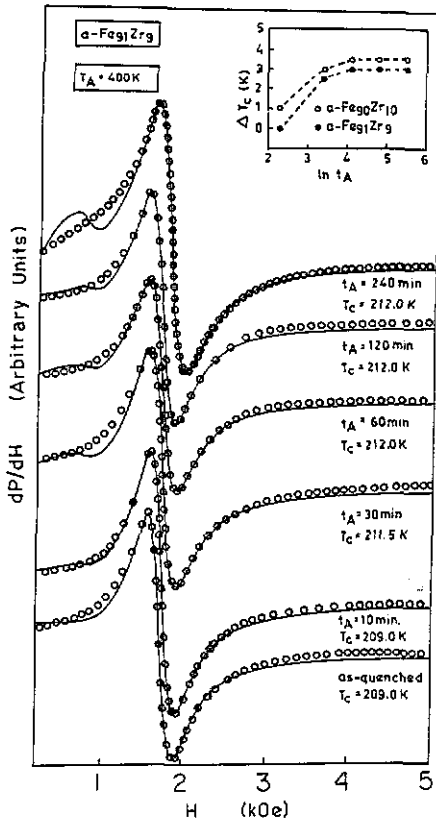


Figure 1. Power absorption derivative curves for $\alpha\text{-Fe}_{91}\text{Zr}_9$ at $T = T_C$ recorded using the \parallel^h sample configuration before and after subjecting this alloy to an isothermal annealing treatment at $T_A = 400$ K for durations of time t_A , ranging from 10 to 240 min. The full curves depict the observed variation whereas the open circles denote the calculated values (see text). The inset shows $\Delta T_C = (T_C)_{\text{annealed}} - (T_C)_{\text{unannealed}}$ plotted against $\ln t_A$.

(ii) While the primary resonance possesses properties characteristic of ferromagnets with re-entrant 'spin-glass-like' behaviour at low temperatures, the secondary resonance exhibits a 'cluster spin-glass-like' behaviour.

(iii) The primary and secondary resonances both originate from the bulk and not from the surface, as inferred from detailed FMR measurements performed on alloy ribbons before and after they have received etching and/or mechanical polishing treatment (Siruguri *et al* 1990).

(iv) Structural relaxation effects are evident in FMR spectra taken for $T \geq 400$ K in that the location and sharpness of the secondary resonance both depend on the length of time the sample is at a given temperature. In view of the last result, the annealing temperature T_A , in the present case, has been fixed at 400 K.

Figure 1 depicts the variation in dP/dH with H in the \parallel^h configuration at $T = T_C$ for $\alpha\text{-Fe}_{91}\text{Zr}_9$ before and after it has undergone isothermal annealing treatment. These curves are also representative of those recorded for $\alpha\text{-Fe}_{91}\text{Zr}_9$ in the \parallel^v configuration and for $\alpha\text{-Fe}_{90}\text{Zr}_{10}$ in both the \parallel^h and the \parallel^v geometries. It is noticed that, as t_A increases, the change, if any, in the H_{res} and ΔH_{pp} for the primary resonance falls well within the error limits whereas the signature of the secondary resonance becomes more pronounced. At temperatures well above T_C (not shown in figure 1), the resonance line centre and linewidth both remain unaltered for the primary resonance while the secondary resonance sharpens with increasing t_A . Now that the principal aim of this investigation is to find out whether or not isothermal annealing has any influence on the critical behaviour

near the FM-to-paramagnetic (PM) phase transition in a-Fe_{90+x}Zr_{10-x} alloys with $x = 0$ and 1, we focus our attention on the primary resonance alone from now onwards. Contrasted with the situation when FMR lines are extremely sharp and the saturation magnetization M_s can be deduced from the observed resonance field by using the resonance condition for the sample geometry in question, FMR lines are generally broad in the critical region and an accurate estimation of H_{res} , M_s and the Landé splitting factor g necessitates a detailed lineshape analysis of each resonance line separately. The observed dP/dH versus H curves (full curves in figure 1) are, thus, fitted to the theoretical expression (Kaul and Siruguri 1987) for dP/dH in the parallel geometry (used in this work) obtained by solving the Landau-Lifshitz-Gilbert (LLG) equation of motion in conjunction with Maxwell's equations, i.e.

$$dP_{\parallel}/dH \propto (d/dH)[(\mu'^2 + \mu''^2)^{1/2} + \mu'']^{1/2} \quad (1)$$

with real and imaginary components of the dynamic permeability given by

$$\begin{aligned} \mu' = \{ & [(H + H_k)(B + H_k) - \Gamma^2 - (\omega/\gamma)^2][(B + H_k)^2 - \Gamma^2 - (\omega/\gamma)^2] \\ & + 2\Gamma^2(B + H_k)(B + H + 2H_k)\} / \{ [(H + H_k)(B + H_k) \\ & - \Gamma^2 - (\omega/\gamma)^2]^2 + \Gamma^2(B + H + 2H_k)^2 \} \end{aligned} \quad (2a)$$

and

$$\begin{aligned} \mu'' = \{ & -2\Gamma(B + H_k)[(H + H_k)(B + H_k) - \Gamma^2 - (\omega/\gamma)^2] + \Gamma(B + H + 2H_k) \\ & \times [(B + H_k)^2 - \Gamma^2 - (\omega/\gamma)^2] \} / \{ [(H + H_k)(B + H_k) \\ & - \Gamma^2 - (\omega/\gamma)^2]^2 + \Gamma^2(B + H + 2H_k)^2 \} \end{aligned} \quad (2b)$$

(in equations (2a) and (2b), $B = H + 4\pi M_s$, H_k is the 'in-plane' uniaxial anisotropy field, $\gamma = g|e|/2mc$, $\Gamma = \lambda\omega/\gamma^2 M_s$ is the linewidth parameter and λ is the Gilbert damping parameter), with the aid of a non-linear least-squares-fit computer program which treats g and M_s as free fitting parameters and uses the observed values of $\Delta H_{\text{pp}} = 1.45\Gamma$ and the values of H_k , deduced from the relations (Conger and Essig 1956)

$$H_{\text{res}}^{\parallel\text{h}} = H_{\text{res}}^{\parallel} - H_k \quad (3a)$$

and

$$H_{\text{res}}^{\parallel\text{v}} = H_{\text{res}}^{\parallel} + H_k \quad (3b)$$

where $H_{\text{res}}^{\parallel\text{h}}$ and $H_{\text{res}}^{\parallel\text{v}}$ are the resonance fields in the \parallel^{h} and \parallel^{v} configurations, respectively, and $H_{\text{res}}^{\parallel}$ is the resonance field in the absence of H_k . The theoretical fits so obtained, depicted by open circles in figure 1, demonstrate that the LLG equation adequately describes the resonant behaviour in the entire range of temperatures and t_A covered in the present experiments. The lineshape calculation, besides revealing that g ($= 2.07 \pm 0.02$) is independent of temperature and/or t_A , yields the variation in H_{res} and M_s with temperature as shown in figures 2 and 3. An important inference from the data presented in these figures is that, at a given temperature, the external field corresponding to M_s is simply H_{res} and both M_s and H_{res} do not exhibit any detectable change with isothermal annealing. Reasonably accurate values of the spontaneous magnetization and initial susceptibility critical exponents β and γ and of T_C are extracted from the $M_s(H_{\text{res}}, T)$ data by identifying H_{res} with the ordering field H conjugate to M ($\equiv M_s$) and using the 'range-of-fit' scaling-equation-of-state (SES) analysis (Kaul 1984,

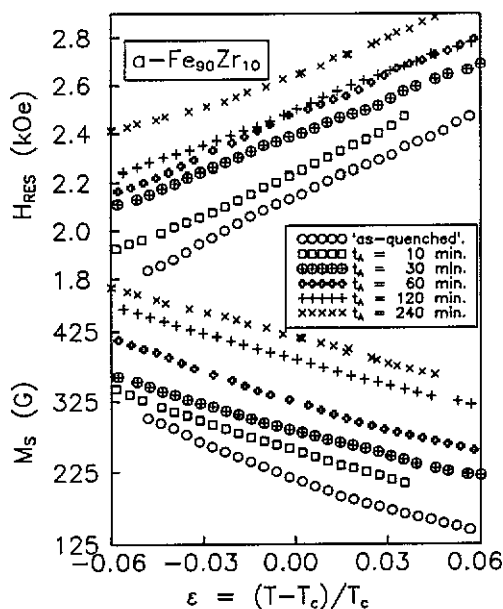


Figure 2. Variation in M_s and H_{res} with reduced temperature for a-Fe₉₀Zr₁₀ deduced from the lineshape analysis. Note that, for clarity, the $M_s(T)$ and $H_{res}(T)$ curves for higher values of t_A have been shifted by 40 G and 100 Oe, respectively, with respect to those corresponding to lower values of t_A .

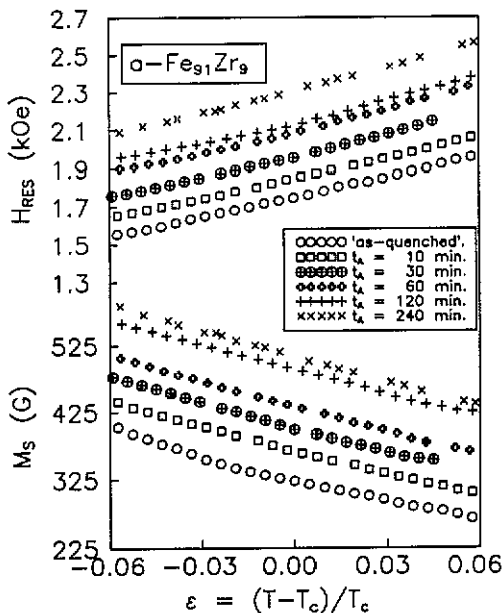


Figure 3. Variation in M_s and H_{res} with reduced temperature for a-Fe₉₁Zr₉ deduced from the lineshape analysis. Note that, for clarity, the $M_s(T)$ and $H_{res}(T)$ curves for higher values of t_A have been shifted by 40 G and 100 Oe, respectively, with respect to those corresponding to lower values of t_A .

1985, Föhnle *et al* 1987, Kaul and Babu 1991) based on the magnetic equation of state $m = f_{\pm}(h)$, where the minus and plus signs refer to temperatures below and above T_C , and $m \equiv M/|\varepsilon|^{\beta}$ and $h \equiv H/|\varepsilon|^{\beta+\gamma}$ are the scaled magnetization and scaled field, respectively. Figure 4 shows scaling plots for a-Fe₉₀Zr₁₀ at different values of t_A and compares the recent bulk magnetization (BM) data (Kaul and Babu 1991) with the FMR data on 'as-quenched' samples from the same batch. Similar scaling plots for the a-Fe₉₁Zr₉ alloy sample before and after it has undergone isothermal annealing at $T_A = 400$ K for different durations of time are depicted in figure 5. Note that the modified asymptotic analysis (Kaul 1984, 1985), employed in the BM case determines the exponents β ($= 0.36 \pm 0.02$) and γ ($= 1.38 \pm 0.03$), and Curie temperature T_C (238.50 ± 0.05 K) to much greater accuracy (Kaul 1984, 1985) than the 'range-of-fit' SES analysis used in the present case, which yields values for β , γ and T_C accurate to within 8%, 4% and 0.1%, respectively.

3. Discussion

Table 1 compares the values of exponents β and γ deduced from the FMR data with those extracted from the previous bulk magnetization and AC susceptibility χ_{ac} measurements on the same and/or different samples cut from the same a-Fe₉₀Zr₁₀ or a-Fe₉₁Zr₉ alloy ribbon. It is evident from the scaling plots (figures 4 and 5) and from the data presented in table 1 that

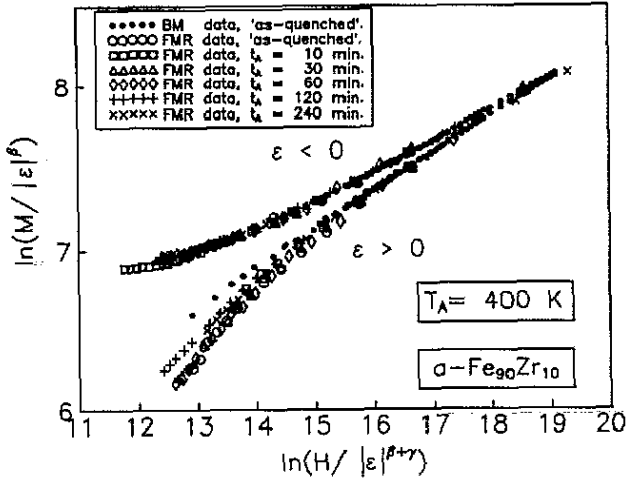


Figure 4. Plots of $\ln(M/|\epsilon|^\beta)$ against $\ln(H/|\epsilon|^{\beta+\gamma})$ for 'as-quenched' and annealed samples of the α -Fe₉₀Zr₁₀ alloy.

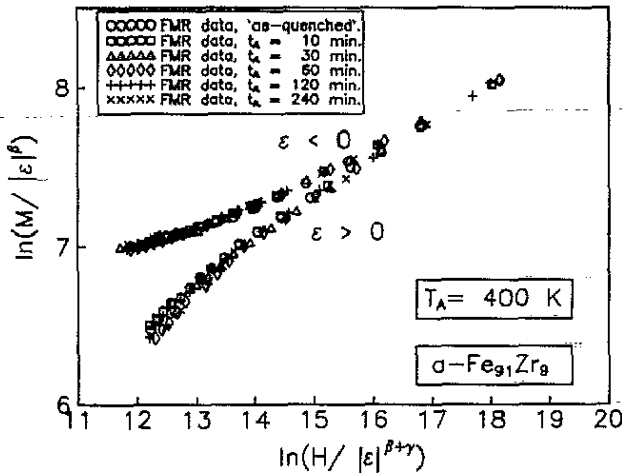


Figure 5. Plots of $\ln(M/|\epsilon|^\beta)$ against $\ln(H/|\epsilon|^{\beta+\gamma})$ for 'as-quenched' and annealed samples of the α -Fe₉₁Zr₉ alloy.

(a) the different sets of FMR data in the 'as-quenched' and annealed conditions fall on two *universal* curves $f_-(h)$ for $\epsilon < 0$ and $f_+(h)$ for $\epsilon > 0$,

(b) consistent with the predictions of the infinite-3D-FM-matrix plus finite-spin-cluster model, the isothermal annealing has *no effect* on the critical behaviour near the FM-to-FM phase transition and hence the transition at T_C is a true phase transition in the thermodynamic sense (alternatively, the structural relaxation caused by annealing treatment, as inferred by a significant increase in T_C with t_A (inset of figure 1), leaves the critical exponents β and γ unaltered (table 1)) and

(c) the exponent values determined in this work conform very well not only with those deduced from BM and χ_{ac} data by employing methods of analysis different from the present method but also with the 3D Heisenberg values.

Table 1. Comparison between the values of critical exponents β , γ and δ determined by different experimental techniques for the 'as-quenched' samples of α -Fe_{90+x}Zr_{10-x} alloys with $x = 0$ and 1 and the effect of isothermal annealing on the critical exponent values: AA, asymptotic analysis (for a detailed description of methods AA-II and AA-II' see Kaul (1985)); ACS, AC susceptibility; BM, bulk magnetization; FMR, ferromagnetic resonance; RG, renormalization group; SES, scaling-equation-of-state analysis (for details of this method see Kaul (1985)); AO, 'as-quenched' sample. The numbers in parentheses denote the uncertainty in the least significant figure.

Alloy composition	Reference	Method	t_A (min)	T_c (K)	β	γ	δ_{obs}	$\delta_{calc} = 1 + \gamma/\beta$	
Fe ₉₀ Zr ₁₀	a	BM, SES	AO	207.50(40)	0.395(20)	1.441(72)	4.686(230)	4.648(368)	
	b	BM, AA-II'	AO	233.00(5)	0.360(20)	1.360(30)	4.780(30)	4.778(294)	
	b	ACS, SES	AO	233.00(5)	—	—	4.800(200)	—	
	c	BM, AA-II'	AO	238.50(5)	0.360(20)	1.380(30)	4.826(35)	4.833(297)	
	d	FMR, SES	AO	238.55(25)	0.380(30)	1.380(60)	—	4.632(447)	
	d	FMR, SES	10	239.50(25)	0.370(30)	1.390(60)	—	4.757(470)	
	d	FMR, SES	30	241.50(25)	0.370(30)	1.390(60)	—	4.757(470)	
	d	FMR, SES	60	242.00(25)	0.370(30)	1.390(60)	—	4.757(470)	
	d	FMR, SES	120	242.00(25)	0.370(30)	1.380(60)	—	4.730(468)	
	d	FMR, SES	240	242.00(25)	0.360(30)	1.380(60)	—	4.833(490)	
	Fe ₉₁ Zr ₉	b	BM, AA-II	AO	202.00(50)	0.360(20)	1.360(30)	4.780(40)	4.778(294)
		b	ACS, SES	AO	210.05(5)	—	—	4.800(200)	—
c		ACS, AA	AO	212.38(5)	—	1.360(30)	—	—	
e		ACS, AA	AO	213.91(10)	—	1.380(50)	—	—	
d		FMR, SES	AO	209.00(25)	0.370(30)	1.380(60)	—	4.730(468)	
d		FMR, SES	10	209.05(25)	0.370(30)	1.380(60)	—	4.730(468)	
d		FMR, SES	30	211.50(25)	0.370(30)	1.380(60)	—	4.730(468)	
d		FMR, SES	60	212.00(25)	0.380(30)	1.380(60)	—	4.632(447)	
d		FMR, SES	120	212.00(25)	0.370(30)	1.380(60)	—	4.730(468)	
d		FMR, SES	240	212.00(25)	0.370(30)	1.390(60)	—	4.757(470)	
3D Heisenberg		f	RG	—	—	0.365(3)	1.386(4)	4.800(40)	—

^a Reisser *et al* (1988).
^b Kaul (1988).
^c Kaul and Babu (1991).
^d Present work.
^e Kaul *et al* (1986).
^f Le Guillou and Zinn-Justin (1980).

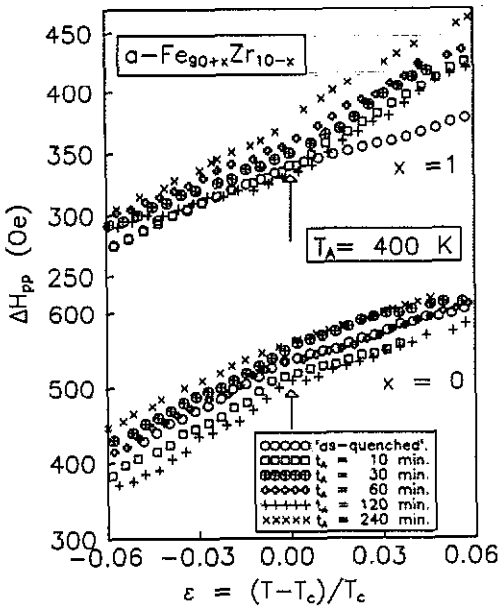


Figure 6. Variation ΔH_{pp} with T in the critical region for 'as-quenched' and annealed samples of the $a\text{-Fe}_{90}\text{Zr}_{10}$ and $a\text{-Fe}_{91}\text{Zr}_9$ alloys. The upward arrows highlight the slope change at $T = T_c$.

In addition, figure 4 demonstrates that excellent agreement exists between the different sets of FMR data and BM results for $\epsilon < 0$ but this agreement is offset for $\epsilon \geq 0.1$ where the former sets of data increasingly deviate from (lie consistently lower than) the latter set. A tentative explanation for this discrepancy between the BM and FMR data can be offered in terms of the *infinite*-3D-FM-matrix plus *finite*-spin-clusters model (Kaul 1984, 1985) as follows. Within the framework of this model, the spins constituting the FM matrix and those forming the finite clusters give rise to the primary and secondary resonances, respectively (for details see Kaul and Siruguri (1991)). As the temperature is raised above T_c , an increased number of spins, originally belonging to the FM matrix, become polarized by the spins within the finite clusters and the clusters grow in size. As a consequence of the reduced number of spins and increased randomness in the spin arrangement in the PM matrix, the primary-resonance field yields a reduced value of M_s compared with the BM case in which all the spins (contained in the finite clusters and the remaining PM matrix) contribute to DC magnetization (for details see Kaul and Siruguri (1991)). Figure 6 displays the variation in ΔH_{pp} with T in the critical region. An abrupt slope change noticed at T_c for both the 'as-quenched' and the annealed samples indicates a sudden release of magnetic entropy at T_c and hence provides additional evidence for a well defined magnetic phase transition at T_c .

4. Summary

The FMR technique yields values for the critical exponents β and γ for the $a\text{-Fe}_{90}\text{Zr}_{10}$ and $a\text{-Fe}_{91}\text{Zr}_9$ alloys that are in excellent agreement not only with those previously determined from bulk magnetization (Kaul 1988) and AC susceptibility (Kaul *et al* 1986, Kaul 1987, 1988) measurements on 'as-quenched' samples but also with those

theoretically predicted (Le Guillou and Zinn-Justin 1980) for a 3D isotropic nearest-neighbour Heisenberg ferromagnet. In conformity with the predictions of the 3D-infinite-FM-matrix plus finite-spin-cluster model (Kaul 1984, 1985), the exponents β and γ are not affected by isothermal annealing which otherwise causes a significant enhancement in the value of the Curie temperature.

Acknowledgments

This work was supported by grant SP/S2/M21/86 from the Department of Science and Technology, New Delhi. One of us (ChVM) is grateful to the University Grants Commission, New Delhi, for granting him a Junior Research Fellowship.

References

- Conger R L and Essig F C 1956 *Phys. Rev.* **104** 915
Fähnle M, Kellner W U and Kronmüller H 1987 *Phys. Rev. B* **35** 3640
Kaul S N 1984 *IEEE Trans. Magn.* **MAG-20** 1290
— 1985 *J. Magn. Magn. Mater.* **53** 5
— 1987 *J. Appl. Phys.* **61** 451
— 1988 *J. Phys. F: Met. Phys.* **18** 2089
Kaul S N and Babu P D 1991 *Phys. Rev. B* at press
Kaul S N, Bansal C, Kumaran T and Havalgi M 1988 *Phys. Rev. B* **38** 9248
Kaul S N, Hofmann A and Kronmüller H 1986 *J. Phys. F: Met. Phys.* **16** 365
Kaul S N, Mohan Ch V, Babu P D, Sambasiva Rao M and Lucinski T 1990 unpublished
Kaul S N and Siruguri V 1987 *J. Phys. F: Met. Phys.* **17** L255
— 1991 *J. Phys.: Condens. Matter* submitted
Le Guillou L C and Zinn-Justin J 1980 *Phys. Rev. B* **21** 3976
Reisser R, Fähnle M and Kronmüller H 1988 *J. Magn. Magn. Mater.* **75** 45
Rhyne J J, Erwin R W, Fernandez-Baca J A and Fish G E 1988 *J. Appl. Phys.* **63** 4080
Ryan D H, Coey J M D, Batalla E, Altounian Z and Ström-Olsen J O 1987 *Phys. Rev. B* **35** 8630
Saito N, Hiroyoshi H, Fukamichi K and Nakagawa Y 1986 *J. Phys. F: Met. Phys.* **16** 911
Shirakawa K, Ohnuma S, Nose M and Masumoto T 1980 *IEEE Trans. Magn.* **MAG-16** 910
Siruguri V, Mohan Ch V and Kaul S N 1990 unpublished